

## Absorption and Fluorescence Spectra of Uracil in the Gas Phase and in Aqueous Solution: A TD-DFT Quantum Mechanical Study

Roberto Improta<sup>\*,†,‡</sup> and Vincenzo Barone<sup>†</sup>

*Dipartimento di Chimica, Università Federico II, Complesso Universitario Monte S. Angelo, Via Cintia, I-80126 Napoli, Italy, and Istituto di Biostrutture e Bioimmagini-CNR, Via Mezzocannone 6 I-80134 Napoli, Italy*

Received July 2, 2004; E-mail: roberto@lsdm.dichi.unina.it

In recent years the excited states of nucleic acid bases have been characterized by several time-resolved fluorescence studies that agree in assigning subpicosecond lifetimes to  $S_1$ , implying very efficient internal conversion processes.<sup>1–3</sup> Unfortunately, while most of the available experimental results have been obtained in condensed phases,<sup>1</sup> none of the few computational papers including solvent effects<sup>4</sup> takes into account at the same time bulk and specific cybotactic contributions. Both effects are instead included in the present study of the absorption and fluorescence spectra of uracil in the gas phase and in solution, which reports to the best of our knowledge the first fluorescence spectra computed in aqueous solution at an accurate quantum mechanical level. We show that (i) the  $S_1/S_2$  ordering strongly depends on the nature of the embedding medium, thus suggesting a possible explanation for the available experimental results<sup>5–12</sup> and (ii) by only taking into account both bulk effects and the cybotactic region it is possible to reproduce solvent effects on the energy and the intensities of the electronic spectra, especially for  $\pi/\pi^*$  transitions.

The spectrum computed in the gas phase at the TD-PBE0 level<sup>13</sup> (see Table 1 and Supporting Information) is in remarkable agreement with experiments<sup>6</sup> and CASPT2 calculations,<sup>14</sup> concerning both positions and intensities of absorptions. As a matter of fact, all the computed vertical excitation energies (VEE) are within 0.1 eV from their experimental counterparts,<sup>6</sup> except for a blue-shifting of the  $S_0 \rightarrow S_2$  transition by  $\sim 0.2$  eV. This latter is better reproduced by CASPT2 calculations,<sup>14</sup> probably because of an overstabilization of  $\pi$ -bonding orbitals by DFT calculations. As for the relative intensities, our picture is very similar to the experimental one, with a weaker band at  $\sim 6$  eV between two strong bands of similar intensities at  $\sim 5.2$  eV and  $\sim 6.6$  eV. In agreement with previous results, the  $S_0 \rightarrow S_1$  transition has an HOMO-1  $\rightarrow$  LUMO ( $n/\pi^*$ ) character (see Figure S1), mainly involving  $C_4-O_8$  carbonyl group (see Figure 1 for atom labeling), whereas the  $S_0 \rightarrow S_2$  transition has a HOMO-LUMO  $\pi/\pi^*$  character (hereafter  $\pi/\pi^*A$ ).

The optimized structures of the  $S_1$  and  $S_2$  states in the gas phase (see Supporting Information) show that the most relevant geometry changes involve the bond lengths, without significant distortion of the ring from planarity. The computed fluorescence peaks should occur at 3.57 and 4.22 eV for the  $S_1$  and  $S_2$  states, respectively. The experimental 0–0 transition energy in supersonic jet is 4.37 eV,<sup>7</sup> in nice agreement with the prediction of our computations for the  $S_0 \rightarrow S_1$  transition (4.23 eV, see Table 1). In the gas phase, the fluorescence emission should thus occur from a dark  $n/\pi^*$  state, in agreement with experimental results for the very similar thymine molecule.<sup>15</sup> Our calculations predict the presence of a very weak maximum at  $\sim 3.57$  eV, which is consistent with the experimental estimate obtained for thymine (3.0–3.3 eV).<sup>15</sup> To take solvent effect into the proper account, we use a cluster including four explicit water molecules (according to both experimental<sup>15,16</sup> and compu-

**Table 1.** Lowest Energy (in eV) Transition (Energy Relative to the Corresponding  $S_0$  Minimum) of Uracil<sup>a</sup>

	$n/\pi^*$	$\pi/\pi^*A$
Absorption		
gas phase	4.80(0.00)	5.26(0.14)
ethanol <sup>b</sup> -PCM	5.15(0.0)	5.20(0.19)
uracil + 4 H <sub>2</sub> O <sup>c</sup>	4.97(0.00)	5.26(0.14)
water-PCM	5.09(0.00)	5.17(0.19)
water-PCM + 4 H <sub>2</sub> O	5.28(0.00)	5.16(0.20)
Emission		
gas phase	4.23(0.00)3.57	5.01(0.04)4.22
ethanol <sup>b</sup> -PCM	4.62(0.00)4.10	5.13(0.11)4.51
water-PCM	4.64(0.00)4.10	4.93(0.20)4.61
water-PCM + 4 H <sub>2</sub> O	4.78(0.00)4.24	4.86(0.20)4.58

<sup>a</sup> TD-PBE0/6-311+G(2d,2p)/PBE0/6-31G(d) calculations. Oscillator strengths are in parentheses. Fluorescence energies are reported in italics. <sup>b</sup> PCM single-point calculations on gas-phase optimized geometries. <sup>c</sup> Gas-phase calculations.

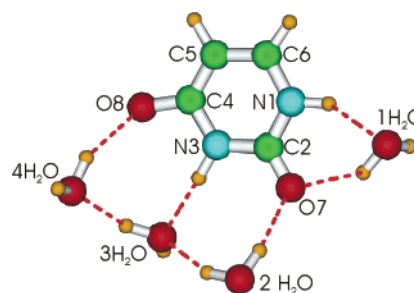


**Figure 1.** Model used for the calculation in aqueous solution: Uracil + four water molecules inserted in a cavity within the continuum.

tational<sup>17</sup> indications; see Supporting Information), which are further embedded in the dielectric continuum mimicking bulk solvent (see Figure 1). UV spectra in solution have been calculated by using the TD-PCM method.<sup>18,19</sup>

While solvent effects on the  $S_0$  equilibrium geometry are modest (see Supporting Information), solvent shifts of the absorption maxima are significant (see Table 1 and Supporting Information). At the highest level of the theory (see Supporting Information) the very weak  $n/\pi^*$  transition is blue-shifted by  $\sim 0.5$  eV, while the strong  $\pi/\pi^*$  transition is red-shifted by  $\sim 0.2$  eV and is predicted to be slightly more intense. As a consequence, in aqueous solution the lowest energy transition is predicted to have a  $\pi/\pi^*$  character, reversing the state ordering predicted in the gas phase. The  $S_3$  and  $S_4$  transitions (both with  $\pi/\pi^*$  character) get much closer with respect to the gas phase, their energy gap being smaller than 0.1 eV. The experimental absorption spectra predict the existence of two broad bands, the first centered around 4.8 eV ( $\epsilon = 8100$ ) and the second at  $\sim 6.1$  eV ( $\epsilon = 8800$ ),<sup>9,10</sup> which could result from the merging of the very close  $S_3$  and  $S_4$  transitions. The  $\pi/\pi^*A$  transition energy is underestimated by  $\sim 0.25$  eV by our approach. PCM computations on the cluster of Figure 1 provide a good estimate of solvent effects both on the energy and on the intensity

<sup>†</sup> Università Federico II, Complesso Universitario Monte S. Angelo.

<sup>‡</sup> Istituto di Biostrutture e Bioimmagini - CNR.

of that transition, whose intensity increases with the polarity of the embedding medium. Our results (see Table 1 and Supporting Information) show that a more reliable computation of solvent shifts in absorption spectra requires the contemporary consideration of bulk solvent effect and specific interactions with water molecules belonging to the first solvation shell. As a matter of fact, coordination of four water molecules, though leading to a remarkable blue shift ( $\sim 0.2$  eV) of the  $n/\pi^*$  transition, is able to provide only 50% of the total solvent shift. Bulk solvent effects are even more important for  $\pi/\pi^*$  transitions, whose energies and, especially, intensities are not significantly affected by the coordination of water molecules in gas-phase calculations. On the other hand, the coordination of solvent molecules significantly affects the energy of carbonyl oxygen lone pair orbitals, while their influence on the diffuse  $\pi$  and  $\pi^*$  orbitals is much more limited. As a consequence, only when solvent molecules are explicitly included,  $\pi/\pi^*$ A becomes the lowest energy transition. Solvent effects on the equilibrium geometry of the  $n/\pi^*$  state are not very large (see Supporting Information), influencing mostly the geometry of the  $N_3-C_4-O_8$  amide group. The elongation of the  $C_2-O_7$  bond and the contemporary shortening of the  $N_1-C_2$  bond are more evident. The geometry of the  $\pi/\pi^*$ A state is instead more affected by the inclusion of solvent effects by the PCM. The weight of the  $C_5, C_6$  atomic orbitals in the molecular  $\pi$  orbitals involved in the transition increases with respect to the gas-phase results. As a consequence, the effect on the  $C_5-C_6$  bond length of the  $\pi/\pi^*$ A transition is larger.

The most significant results obtained by the excited-state geometry optimizations in aqueous solution concern the dependence of the hydrogen bond distances on the electronic state. For the optimized  $n/\pi^*$  solvation shell, the  $H_{w4}-O_8$  hydrogen bond distance is significantly longer (by  $\sim 0.2$  Å) than in the ground electronic state. This electronic transition decreases the electron population of the  $O_8$  lone pairs, leading to a weakening of the hydrogen bond involving the  $C_4-O_8$  carbonyl group. For the  $\pi/\pi^*$ A state, the most relevant change involves instead  $1-H_2O$ , remarkably increasing the  $H_{w1}-O_7$  hydrogen bond length in order to optimize the  $O_{w1}-H_1$  hydrogen bond strength. Not only do the hydrogen bond distances decrease by  $\sim 0.1$  Å, but also the hydrogen bond adopts a linear optimal arrangement.

The predicted Stokes shift in ethanol solution for the  $\pi/\pi^*$ A transition is in nice agreement with the experimental results (0.6 eV) obtained in methanol/ethanol mixed solvent.<sup>5</sup> The agreement found in aqueous solution is slightly worse, though still satisfactory, the experimental Stokes shift ( $\sim 0.8$  eV)<sup>10-12</sup> being larger than the computed one ( $\sim 0.6$  eV). Interestingly, the  $n/\pi^*$  state, which is less stable than the  $\pi/\pi^*$ A state at the equilibrium geometry of the ground state (i.e., in the absorption spectrum), is predicted to be the lowest energy emitting state. The most significant geometry change involves indeed the carbonyl group and suffers from geometrical ring constraints less than  $\pi/\pi^*$ A. On the other hand, the predicted energy difference between the two minima is  $\sim 0.1$  eV and, thus,  $\pi/\pi^*$ A should be the lowest energy minimum, since we have seen that our computations underestimate its energy by  $\sim 0.2$  eV. However, independently of the energy ordering, our computations predict that the energy difference between  $n/\pi^*$  and  $\pi/\pi^*$ A states in polar solvents is very small ( $\pm \sim 0.1$  eV), both in absorption and in emission. The results of this study can shed some light on the intriguing behavior of uracil: (i) the fluorescence quantum yield is not vanishing only in hydrogen bonding solvents<sup>5</sup> and (ii) the fluorescence spectrum is the mirror image of the absorption spectrum<sup>10,12</sup> and the anisotropy is very high,<sup>10</sup> suggesting that absorption and emission occur from the same state. In any

case, the fluorescence quantum yield is very low, while the absorption has strongly allowed character (the absorption peak is very intense), and emission from a low-lying forbidden state has been proposed.<sup>12</sup>

In the gas phase and in nonpolar solvents, the lowest energy state is the dark  $n/\pi^*$  state and radiationless decay to the ground state occurs from that state. Only in hydrogen bonding polar solvents does the  $\pi/\pi^*$ A state become the lowest energy state, although its energy is always extremely close to that of the  $n/\pi^*$  state. The ultrafast internal conversion in uracil (lifetimes of  $\sim 200$  fs, the lowest among the nucleobases)<sup>1</sup> can thus be explained on the ground of the "so-called" proximity effect.<sup>20</sup> Solvent could obviously influence other relevant aspects of the uracil excited-state dynamics, as the accessibility of  $S_2/S_1$  and  $S_1/S_0$  conical intersections<sup>21</sup> or the potential energy surface associated to their coupling modes (e.g., the out-of-plane ring deformations of the ring).<sup>4b,21</sup>

According to our results, it would be possible that the arrangement of solvent molecules around uracil plays a relevant role in coupling  $S_1$  and  $S_2$  states. The solvation shell of  $S_1$  and  $S_2$  states is very different, suggesting that their ordering could change following the motion of just a single solvent molecule. Only a dynamical treatment including a larger number of explicit solvent molecules could provide a definite answer to this question, which is difficult to tackle by experiments because of the very different intensity of the two overlapping transitions. However, it is noteworthy that the time scale for solvent equilibration (i.e., 50–200 fs depending on the librational/translational motion of the solvent molecules)<sup>22</sup> is consistent with the order of magnitude of uracil fluorescence lifetime in solution.

**Acknowledgment.** We thank Dr. T. Gustavsson for very useful discussions and MURST for financial support.

**Supporting Information Available:** Equilibrium geometries and relative tables. Computational and methodological details. Results concerning additional excited states. This material is available free of charge via the Internet at <http://pubs.acs.org>.

## References

- (1) Crespo-Hernandez, C. E.; Cohen, B.; Hare, P. M.; Kohler, B. *Chem. Rev.* **2004**, *104*, 1977.
- (2) Ismail, N.; Blancafort, L.; Olivucci, M.; Kohler, B.; Robb, M. A. *J. Am. Chem. Soc.* **2002**, *124*, 6818.
- (3) Merchan, M.; Serrano-Andres, L. *J. Am. Chem. Soc.* **2003**, *125*, 8108.
- (4) (a) Fulscher, M. P.; Serrano-Andres, L.; Roos, B. O. *J. Am. Chem. Soc.* **1997**, *119*, 6168. (b) Shukla, M. K.; Leszczynski, J. *J. Phys. Chem. A* **2002**, *106*, 8642. (c) Broo, A.; Holmen, A. *J. Phys. Chem. A* **1997**, *101*, 3589. (d) Mennucci, B.; Toniolo, A.; Tomasi, J. *J. Phys. Chem. A* **2001**, *105*, 4749. (e) Broo, A.; Pearl, G.; Zerner, M. C. *J. Phys. Chem. A* **1997**, *101*, 2478. (f) Marian, C. M.; Schneider, F.; Kleinschmidt, M.; Tatchen, J. *Eur. Phys. J. D* **2002**, *20*, 357.
- (5) Becker, R. S.; Kogan, G. *Photochem. Photobiol.* **1980**, *31*, 5.
- (6) Clark, L. B.; Peschel, G. G.; Tinoco, I., Jr. *J. Phys. Chem.* **1965**, *69*, 3615.
- (7) Fujii, M.; Tamura, T.; Mikami, N.; Ito, M. *Chem. Phys. Lett.* **1986**, *126*, 583.
- (8) Voet, D. R.; Gratzler, W. B.; Cox, R. A.; Doty, P. *Biopolymers* **1963**, *1*, 193.
- (9) Callis, P. R. *Annu. Rev. Phys. Chem.* **1984**, *34*, 329.
- (10) Williams, S. A.; Renn, C. N.; Callis, P. R. *J. Phys. Chem.* **1987**, *91*, 2730.
- (11) Daniels, M.; Hauswirth, W. *Science* **1971**, *171*, 675.
- (12) Turpin, P. Y.; Peticolas, W. L. *J. Phys. Chem.* **1985**, *89*, 5156.
- (13) Adamo, C.; Scuseria, G. E.; Barone, V. *J. Chem. Phys.* **1999**, *111*, 2889.
- (14) Lorentzon, J.; Fulscher, M. P.; Roos, B. O. *J. Am. Chem. Soc.* **1995**, *117*, 9265.
- (15) He, Y.; Wu, C.; Kong, W. *J. Phys. Chem. A* **2004**, *108*, 943.
- (16) Chahinian, M.; Seba, H. B.; Ancian, B. *Chem. Phys. Lett.* **1998**, *285*, 337.
- (17) Gaigeot, M.-P.; Sprik, M. *J. Phys. Chem. B* **2004**, *108*, 7458.
- (18) Cossi, M.; Barone, V. *J. Chem. Phys.* **2001**, *115*, 4708.
- (19) Cossi, M.; Barone, V. *J. Phys. Chem. A* **2000**, *104*, 10614.
- (20) Lim, E. C. *J. Phys. Chem.* **1986**, *90*, 6770.
- (21) Matsika, S. *J. Phys. Chem. A* **2004**, *108*, 7584.
- (22) Aherne, D.; Tran, V.; Schwartz, B. *J. J. Phys. Chem. B* **2000**, *104*, 5382.

JA0460561